Atmos. Chem. Phys. Discuss., 7, 17179–17211, 2007
www.atmos-chem-phys-discuss.net/7/17179/2007/

Atmospheric Chemistry and Physics Discussions

Ozone-enhanced layers in the troposphere over the equatorial Pacific Ocean and the influence of transport of midlatitude UT/LS air

H. Hayashi[1], K. Kita[1], and S. Taguchi[2]

[1]Department of Environmental Sciences, College of Science, Ibaraki University, Mito, Japan
[2]Research Institute for Environmental Management Technology, National Institute of Advanced Industrial Science and Technology (AIST), Tsukuba, Japan

Received: 12 October 2007 – Accepted: 13 November 2007 – Published: 26 November 2007

Correspondence to: K. Kita (kita@mx.ibaraki.ac.jp)

Abstract

Occurrence of ozone (O_3)-enhanced layers in the troposphere over the equatorial Pacific Ocean and their seasonal variation were investigated based on ozonesonde data obtained at three Southern Hemisphere ADditional OZonesondes (SHADOZ) sites, Watukosek, American Samoa and San Cristobal, for 6 years between 1998 and 2003. O_3-enhanced layers were found in about 50% of observed O_3 profiles at the three sites on yearly average. The formation processes of O_3-enhanced layers were investigated by meteorological analyses including backward trajectories. On numerous occasions, O_3-enhanced layers resulted from the transport of air masses affected by biomass burning. The contribution of this process was about 30% at San Cristobal during the periods from February to March and from August to September, while it was relatively low, about 10%, at Watukosek and Samoa. A significant number of the O_3-enhanced layers were attributed to the transport of midlatitude upper-troposphere and lower-stratosphere (UT/LS) air. Meteorological analyses indicated that these layers originated from equatorward and downward transport of the midlatitude UT/LS air masses through a narrow region between high- and low-pressure systems around the subtropical jet stream. This process accounted for more than 40% at Watukosek between May and December, about 60% or more at Samoa all year around, and about 40% at San Cristobal between November and March, indicating that it was important for O_3 budget over the equatorial Pacific Ocean.

1 Introduction

The tropospheric ozone (O_3) concentration in the tropics is generally low. However, O_3-enhanced layers are often observed there (e.g., Newell et al., 1996; Stoller et al., 1999; Thouret et al., 2001). Photochemical production from the O_3 precursor gases emitted from biomass burning is considered to be a significant cause of relatively high O_3 concentrations in the tropical troposphere. Increases in O_3 associated with biomass

ACPD

7, 17179–17211, 2007

Ozone-enhanced layers in the equatorial troposphere

H. Hayashi et al.

burning over the tropical Pacific Ocean have been repeatedly reported. Oltmans et al. (2001) suggested that the O_3-enhanced layers observed at Fiji (18.1° S, 178.2° E), Samoa (14.3° S, 189.4° E), Tahiti (18.0° S, 211.0° E), and Galapagos (0.9° S, 270.4° E) with ozonesondes were attributable to the transport of air masses affected by biomass burning in Australia and South America. In Indonesia, during the local late dry season between September and November, enhancements of tropospheric O_3 concentrations are often observed (Komala et al., 1996; Fujiwara et al., 2000), and similar O_3 enhancements have also been observed in Malaysia between March and May (Yonemura et al., 2002a). Especially during El Niño periods, when severe droughts and extensive biomass burning occurred in Indonesia, remarkably large O_3 increases have persisted (Fujiwara et al., 1999; Yonemura et al., 2002b). Satellite total O_3 data also showed O_3 increases over the Indonesian region and the Indian Ocean during these periods (Chandra et al., 1998; Kita et al., 2000).

Transport of O_3-abundant air masses is another cause of tropospheric O_3 increases in the tropics. Active convection over Indonesia has been shown to carry O_3 precursors to the upper troposphere, increasing the O_3 concentration over Indonesia, the Indian Ocean and northern Australia (Kita et al., 2002). The downward transport of air masses from the upper troposphere and lower stratosphere (UT/LS) is also suggested to increase the O_3 concentration in the tropics. Fujiwara et al. (1998) observed O_3 enhancement in the upper troposphere at Watukosek (7.57° S, 112.65° E), Indonesia and indicated that the breaking of equatorial Kelvin waves around the tropopause caused O_3 transport from the stratosphere into the troposphere. The intrusions of the midlatitude UT/LS air in association with the breaking of Rossby waves around the subtropical jet stream have been suggested to cause the O_3 increase as well as decrease of humidity in the tropics (e.g., Baray et al., 2000; Scott et al., 2001; Waugh and Funatsu, 2003; Waugh, 2005). Yoneyama and Parsons (1999) found extremely dry layers in the lower and middle troposphere over the tropical western Pacific Ocean, and suggested that they originated from Rossby wave breaking. Zachariasse et al. (2001) found O_3 enhancement with low relative humidity (RH) in the middle troposphere over the Indian

Ocean, and suggested that it was attributed to a pair of anticyclones located along the subtropical jet stream over the western Pacific and Australia. Baray et al. (1998) discussed the possible influences of tropopause foldings near the subtropical jet stream on the tropical tropospheric O_3 concentrations. They showed that tongues of air mass near the subtropical jet stream with high potential vorticity (PV) values extended to the subtropical latitudes in the middle troposphere. Occurrence of intrusions of high-PV air masses, induced by wave-breaking events, were relatively high over the Pacific and Atlantic Oceans during northern winter, when westerly ducts are strongest (e.g., Postel and Hitchman, 1999; Waugh and Polvani, 2000). These studies showed that the high-PV air masses could directly intrude into latitudes of about 20°. However, it is not clear whether the transportation of these air masses to the equatorial region from midlatitude UT/LS directly contributes to O_3 enhancement in this region. Systematic studies on the contribution of the midlatitude UT/LS air intrusions to tropospheric O_3 enhancement in the tropics using long-term observational data have also been quite limited.

In this work, 6-year ozonesonde data at three equatorial sites in the western, central and eastern Pacific Ocean were used to examine the occurrence of O_3-enhanced layers in the free troposphere over this region and its seasonal variations. Contributions of biomass burning and the intrusion of midlatitude UT/LS air masses, as well as their seasonal variations, were examined. The transport process of midlatitude UT/LS air masses into the equatorial region and its importance are also discussed.

2 Ozone and meteorological data

In order to investigate O_3-enhanced layers in the troposphere over the western, central, and eastern Pacific Ocean, we analyzed ozonesonde data obtained at three equatorial stations, Watukosek (7.57° S, 112.65° E), Indonesia, American Samoa (14.23° S, 189.44° E), and San Cristobal (0.92° S, 270.40° E), Galapagos. Figure 1 shows the location of these three sites. In general, ozonesonde observations have been regularly carried out once per week as a part of the Southern Hemisphere ADditional

ACPD

7, 17179–17211, 2007

OZonesondes (SHADOZ) experiment (Thompson et al., 2003a and 2003b), and the data are available at the SHADOZ website (http://croc.gsfc.nasa.gov/shadoz/). The data analyzed in this work were obtained between August 1999 and April 2002 at Watukosek, between January 1998 and March 2003 at Samoa, and between March 1998 and August 2002 at San Cristobal.

In the observation, O_3 concentration and RH were measured with balloon-borne electrochemical concentration cell (ECC) ozonesondes (Science Pump type 6A at Samoa and San Cristobal, and ENSCI type 2Z at Watukosek) with Vaisala RS-80 radiosondes (Oltmans et al., 2001; Fujiwara et al., 2003). Although O_3 data were derived using MEISEI RSII-KC79D ozonesondes between May 1993 and July 1999 (Komala et al., 1996; Fujiwara et al., 2000), these data were not included in this study because RH was not measured during this period. The precision of the O_3 measurements is 5–10% in the troposphere. The measured RH is valid without any corrections down to about -30°C air temperature (e.g., Miloshevich et al., 2001). The vertical resolution of O_3 concentration and RH is less than about 100 m.

In order to investigate the origins and transport routes of the O_3-enhanced air masses, kinematic backward/forward trajectories were calculated. In the calculation, the European Centre for Medium-Range Weather Forecast (ECMWF) gridded data and a computing program developed by Tomikawa and Sato (2005) were used. The spatial and temporal resolution of ECMWF data was $2.5^{\circ} \times 2.5^{\circ}$ and 12 h, respectively. The time step for calculation was 1 h, and the vertical displacement of air masses was calculated using the vertical wind component of the ECMWF data.

PV was used to indicate the transport of the midlatitude UT/LS air to the equatorial region. PV values were calculated from the ECMWF gridded data using a computing program developed by National Institute of Advanced Industrial Science and Technology (AIST). In this program, isentropic surface levels were evaluated from vertical temperature profiles at each grid. The horizontal wind vectors were linearly interpolated to the isentropic surfaces in the vertical direction to calculate PV values from them.

The location of convection, which can upwardly transport air in the planetary bound-

ACPD

7, 17179–17211, 2007

EGU

ary layer (PBL), was inferred using outgoing longwave radiation (OLR) data. National Centers for Environmental Prediction (NCEP) operational OLR data (http://www.cdc.noaa.gov/Composites/Day/) were used in the analysis. The locations of biomass burning, which can emit O_3 precursors, were shown using satellite hot-spot data (spots indicating high temperature) obtained from the World Fire Atlas provided by the European Space Agency (http://dup.esrin.esa.it/ionia/wfa/index.asp) using Along Track Scanning Radiometer (ATSR)-2 data.

3 Results

The tropospheric O_3 concentrations measured at the three sites showed a seasonal variation: at Watukosek, Samoa and San Cristobal, respectively, it was higher in the periods from August to November, June to December and July to November than the periods from December to July, January to May and December to June. Median values and central 66.6% ranges of the observed mixing ratios were separately calculated in each 1-km altitude range between 0 and 12 km during these periods at each station, and are shown in Fig. 2. The median values of O_3 mixing ratios over the equatorial Pacific Ocean were between 20 and 40 ppbv.

When the measured O_3 mixing ratio exceeded its lower 83.3 percentile range in the free troposphere at altitudes below 12 km, we regarded it as an O_3-enhanced layer. If the O_3 enhancement reached altitudes above 12 km, we excluded it from this analysis because of the possibility of its being a direct influence of the tropospheric tropopause layer (TTL), which is connected to the stratosphere. O_3 enhancement near the surface, probably in the PBL, was also excluded because it was considered to be a result of O_3 production in the surface-polluted air. Figure 3a and b show vertical profiles of O_3 mixing ratios and RH at Watukosek on 3 December 2000 and on 7 June 2000, respectively. O_3 mixing ratios obviously exceeded their lower 83.3 percentile range at altitudes between 2 and 6 km in Fig. 3a, and at altitudes between 2.5 and 4 km, between 4.5 and 5.5 km and between 6.5 and 8 km in Fig. 3b, and these altitude ranges are considered to be O_3-enhanced layers. We excluded the cases in which the vertical thickness of the layer was less than about 1 km, such as the layer at about 10.5 km in Fig. 3a, because it is difficult to investigate these small-scale events by trajectory analyses. The increase of O_3 up to about 50 ppbv below 1.5 km in Fig. 3b was also excluded, because it occurred in the PBL.

Figure 4 shows the occurrence of O_3-enhanced layers at the three sites by month. The number of occurrence were calculated by dividing the number of profiles where one or more O_3-enhanced layers appeared by that of the total observed profiles in each month. At these sites, the yearly average of the occurrence was about 50%, indicating that O_3-enhanced layers occurred frequently. The occurrence shows a seasonal variation. At Watukosek, it was about 40% in the periods from January to April and from August to November, while it exceeded about 70% in the other months. At Samoa, it was less than 40% between February and April, while it was about 50% or more from May to January except for August. At San Cristobal, it was less than 30% in April, May and July, while it generally exceeded 50% in other months. These seasonal variations are connected to the processes by which O_3-enhanced layers are formed, as discussed in the next section.

RH in the O_3-enhanced layer is considered an indicator of the vertical displacement of O_3-enhanced air masses. If an O_3-enhanced air mass were raised by convection just before it was observed, its RH would increase and be higher than those at the altitudes above and below the layer. On the contrary, if an O_3-enhanced air mass was transported downward, RH would decrease. Especially, if the O_3-enhanced air mass was transported from the UT/LS region, the RH should be very low. We found that the RH in more than 90% of the O_3-enhanced layers was lower than those in the altitude above and below the layer, as in the three layers shown in Fig. 3b, at all three sites. This result suggests that downward transport of air masses, such as downward transport of the UT/LS air mass, is very important for the formation of O_3-enhanced layers. On the contrary, the RH in the O_3-enhanced layer was higher than those above and below the layer in about 40% of cases in December and January at Watukosek,

ACPD
7, 17179–17211, 2007

and in about 20% of cases in March and October at San Cristobal. This result suggests that upward transport probably due to active convection may produce an O_3-enhanced layer in some cases.

4 Discussion

4.1 Influence of biomass burning

Transport of plumes from biomass burning and the O_3 photochemical production in them is one way the O_3-enhanced layers were assumed to form. If an air mass in an O_3-enhanced layer was transported over a region where active biomass burning occurred, and if convection concurrently occurred near this region to enable the upward transport of the plume from the biomass burning, we inferred that the O_3-enhanced layer resulted from the biomass burning. As shown in the vertical profiles of O_3 mixing ratio and RH in Fig. 3a, an O_3-enhanced layer was observed at altitudes between 3.5 and 6 km at Watukosek on 3 December 2000. The RH also increased in this layer. Figure 5 shows 10-day backward trajectories calculated from nine grid points around Watukosek at 550 hPa (about 5 km) from the measurement time. A major part of the trajectories show that the air mass was transported from the boundary layer over northern Australia as shown by red curves. Higher RH in this layer is consistent with this result. Figure 6 shows that there were many hot spots in northern and eastern Australia during the period when the trajectories passed over this region, indicating that biomass burning was active there. Figure 7 is a contour map of the daily average OLR value on 30 November, when the trajectories suggested a rapid upward transport in the northern Australia, and the OLR values were significantly low over this region, implying that active convection occurred there. These results strongly suggest that O_3 precursors emitted from biomass burning over northern Australia were upwardly transported by convection over the northwest of this region, and that O_3 photochemical production during the transport formed the O_3-enhanced layer found over Watukosek.

ACPD

7, 17179–17211, 2007

Ozone-enhanced layers in the equatorial troposphere

H. Hayashi et al.

EGU

In this way we categorized O_3-enhanced layers resulting from biomass burning from the evidence of backward trajectories, hot spot maps, and OLR values. Figure 8a, b and c shows the number of O_3-enhanced layers observed at Watukosek, Samoa, and San Cristobal, respectively, in each month. The number of layers resulting from biomass burning is shown by black bars. The contribution of biomass burning was relatively large (about 30%) at San Cristobal during the periods from February to April and from August to September, probably due to the influence of biomass burning in South America. At Watukosek and Samoa, it was relatively small (less than 10%). The small contribution of biomass burning in the western Pacific region was partly because biomass burning was inactive over this region including Indonesia between 1998 and 2002, when the La Niña tendency dominated. Significant O_3 increases in this region were reported in the El Niño periods.

4.2 Influence of the transport of midlatitude UT/LS air

Because of the frequent stratosphere-troposphere exchange, active O_3 photochemical production in the urban polluted air, and less O_3 destruction due to lower water vapor concentration, the O_3 concentration in the midlatitude is generally higher than that in the tropics. The transport of midlatitude UT/LS air can form O_3-enhanced layers with significantly low RH in the tropical middle troposphere.

As shown in the vertical profiles of the O_3 mixing ratio and RH in Fig. 3b, O_3-enhanced layers at altitudes between 2.5 and 4 km, between 4.5 and 5.5 km and between 6.5 and 8 km, were observed at Watukosek on 7 June 2000. The RH negatively correlated with O_3 in these layers. Figure 9a shows nine 10-day backward trajectories calculated from the center layer at 550 hPa (about 5 km) from the measurement time. Backward trajectories calculated from upper (about 7 km) and lower (about 3.5 km) layers were similar to those in Fig. 9a. The trajectories can be categorized into two groups: trajectories coming from a region along the subtropical jet stream at about 25° S over the Indian Ocean (shown by red curves) and those coming from eastern Indonesia/north of Australia (shown by blue curves). The former trajectories show a

ACPD
7, 17179–17211, 2007

downward motion from about the 300 hPa level, and the latter trajectories show an upward motion from the PBL (not shown). Low-RH values in this layer are consistent with the former trajectories, indicating that the air masses in these layers were transported eastward along the subtropical jet stream at about 25° S several days and were transported equatorward and downward after that.

As shown in Sect. 3, O_3-enhanced layers with low RH, similar to those in Fig. 3b, accounted for about 90% of all O_3-enhanced layers observed at the three sites. Backward trajectory analysis indicates that a significant part of these O_3-enhanced layers with low RH were attributed to the transport of midlatitude UT/LS air. Figure 9b–d shows representative examples of 10-day backward trajectories calculated from these layers, showing that the high-O_3, low-RH air masses observed in these layers were transported from latitudes higher than 20° near the subtropical jet stream and from altitudes higher than the 300 hPa level to the equatorial middle troposphere. No low-OLR region was found along the trajectories (not shown), implying that convection did not affect these air masses. We considered the O_3-enhanced layers with similar trajectories and without a low-OLR region along them to result from the transport of midlatitude UT/LS air.

Red bars in Fig. 8a–c show the number of layers resulting from the transport of midlatitude UT/LS air, indicating that this process significantly contributed to the formation of O_3-enhanced layers in the equatorial Pacific region. At Watukosek, about 40% or more of the O_3-enhanced layers were attributed to this process in the periods from June to September and from November to December. At Samoa, this process accounted for a major part of the O_3-enhanced layers throughout the year, and the contribution of this process was about 75% on yearly average. At San Cristobal, the O_3-enhanced layers resulting from this process contributed about 40% or more in the period from November to March, and their contribution was significant in the period from August to September. Seasonal variation in the contribution of this process would be connected with the transport process (or transport route) of the midlatitude UT/LS air, as discussed in the next subsection.

ACPD

7, 17179–17211, 2007

EGU

The formation process of the other O_3-enhanced layers, which did not result from biomass burning or transport of midlatitude UT/LS air, remains uncertain. Trajectories calculated from these layers show that the high-O_3, low-RH air masses in these layers were transported from the upper troposphere in the tropics. These air masses might have resulted from subsidence of TTL air or mixing of TTL air. Otherwise, they might have been affected by the upward transport of plume from biomass burning or by the abundant nitric oxide (NO) produced by lightning discharge.

4.3 The transport process of the midlatitude UT/LS air to the equatorial region

In order to understand the transport process of the midlatitude UT/LS air masses to the equatorial Pacific region, we investigated the transport route of the air masses and connections with the meteorological condition by using the data derived in 2000. We have adopted absolute PV (|PV|) values larger than 1 PV unit (PVU: $1\,PVU=10^{-6}\,m^2\,s^{-1}\,K\,kg^{-1}$) to indicate the midlatitude UT/LS air. Figure 10 is a contour map of PV on the 327 K isentropic surface on 5 June 2000, 2 days before the layer was observed at Watukosek. The trajectory shown in Fig. 9a show that the air mass in the O_3-enhanced layer in Fig. 3b at 5 km was located at about 20° S near the subtropical jet stream at 327 K. Although high |PV| air masses projected into the tropics about 17° S latitude and 120° E longitude, no high |PV| values calculated from the ECMWF data were found near the equator even when the O_3-enhanced layer was observed over Watukosek.

Figure 11 shows the 3-day forward trajectories indicating the transport of |PV|=1 PVU air masses. Black dots indicate the position of the air masses at longitudinal intervals of 1.125° between 75° E and 130° E on 5 June. The trajectories calculated from these positions suggest that the transport of the midlatitude UT/LS air masses could be categorized into two groups: air masses west of 92° E and north of 21° S are transported equatorward and downward to Indonesia including Watukosek by a counterclockwise flow as shown by red curves, and the other air masses are transported eastward along the winding subtropical jet stream. The former result is consistent with the backward

ACPD
7, 17179–17211, 2007

trajectories in Fig. 9a.

Figures 12 and 13 are wind fields and contour maps of the geopotential height at 400 hPa on 5 June around Indonesia, respectively. They suggest that the counter-clockwise flow was due to the circulation around a high-pressure system in the west of northern Australia, roughly at (15° S, 95° E), and that the winding of the subtropical jet stream was due to a low-pressure system over central Australia. The equatorward trajectories show that the midlatitude UT/LS air was transported into the equatorial region by way of a narrow region between high- and low-pressure systems. The air temperature, RH and vertical pressure velocity over the same region at the same pressure level (not shown) indicated the downward transport of dry and cold air through this region, being consistent with the downward transport of the midlatitude UT/LS air toward the equator. These meteorological characteristics in association with the transportation of midlatitude UT/LS air into the equatorial middle troposphere, a dry, cold air mass with high |PV|, and high O_3 subsided and intruded through the region between the high- and low-pressure systems in UT near the subtropical jet stream, are analogous to those connected with the intrusion of stratospheric air in the midlatitude (e.g., Palmen and Newton, 1969) by Rossby wave breaking around the jet stream.

Figure 14a schematically illustrates the transportation process of the midlatitude UT/LS air near Watukosek during the dry season between May and October. The solid curves with arrows are forward trajectories calculated from 13 June 2000, 1 day before an O_3-enhanced layer was observed at Watukosek. During the dry season, a steady high-pressure system exists over western Australia in association with the subsidence phase of the Hadley cell. When a low-pressure system develops east of this high-pressure system in the middle and upper troposphere, the subtropical jet stream winds north and south as shown by the dotted curve, and the midlatitude UT/LS air mass is intruded equatorward and downward toward Watukosek through the region between the high- and low-pressure systems. Figure 14b similarly illustrates the transportation process near Watukosek in the wet season, between November and December. The solid curves with arrows are forward trajectories calculated from 3 December 2000, 6 days before an O_3-enhanced layer was observed at Watukosek. In the wet season, a steady low-pressure system exists over northern Australia. When a high-pressure system developing over the Indian Ocean at about 17° S extends eastward and a low-pressure system develops south-east of this high-pressure system at about 28° S, the midlatitude UT/LS air mass was intruded equatorward and downward over the Indian Ocean at about 100° E through the region between these high- and low-pressure systems. After that, the midlatitude UT/LS air mass was transported eastward to Watukosek by cyclonic circulation around the low-pressure system over northern Australia. From January to April, transport of the midlatitude UT/LS air seldom occurred at Watukosek.

Transport of the midlatitude UT/LS air occurs more frequently at Samoa than that at the other sites, probably because it is located near the subtropical jet steam. As shown in Fig. 14c, a high-pressure system exists over the south-west of Samoa, roughly at 175° E, all the year around. The solid curves with arrows are forward trajectories calculated from 15 May 2000, 4 days before an O_3-enhanced layer was observed at Samoa. As with Watukosek, the midlatitude UT/LS air mass was transported to Samoa when a low-pressure system occurred in the east of the high-pressure system.

At San Cristobal, the midlatitude UT/LS air is transported from the northern or southern hemisphere, depending on the positions of the intertropical convergence zone (ITCZ) and the subtropical jet stream. Figures 14d and e are schematic illustrations of the transportation process of the midlatitude UT/LS air near San Cristobal in the periods from August to September, and from February to March, respectively. The solid curves in these figures are forward trajectories calculated from 18 February and 15 August, respectively, 2000, 6 days and 9 days before an O_3-enhanced layer was observed at San Cristobal. From February to March, the northern subtropical jet stream runs close to San Cristobal. When a high-pressure system exists over Central America at about 15° N and a low-pressure system exists north-east of the high-pressure system, the midlatitude UT/LS air is intruded equatorward and downward at around 280° E and is transported westward toward San Cristobal by anticyclonic circulation. Between August and September, the austral subtropical jet stream runs close to San Cristobal. When the high-pressure system exists over South America at about 15° S, 300° E and the low-pressure system exists in the south-east of the high-pressure system, the midlatitude UT/LS air is intruded equatorward and downward through the region between the high- and low-pressure systems around 315° E and is transported toward San Cristobal. Figure 14f similarly illustrates the transportation process of the midlatitude UT/LS air in the period from November to January. The solid curves in figure are forward trajectories calculated from 5 December 2000, 9 days before an O_3-enhanced layer was observed at San Cristobal. In this period, the midlatitude UT/LS air is often intruded equatorward and downward into the middle and upper troposphere through the region between high- and low-pressure systems over the northern central Pacific Ocean roughly at 20° N and 180° E. The intrusion of the midlatitude UT/LS air often occurs between high- and low-pressure systems over the southern central Pacific Ocean roughly at 20° S and 180° E. After the intrusion, the midlatitude UT/LS air is transported eastward to San Cristobal. In May, June, July, and October, the transport of midlatitude UT/LS air seldom occurred at San Cristobal.

5 Summary

Ozonesonde data obtained in the western (Watukosek), central (Samoa) and eastern (San Cristobal) Pacific Ocean were analyzed to discuss the occurrence of O_3-enhanced layers in the troposphere over the equatorial Pacific Ocean and their formation processes. The median and lower 83.3% percentile values of O_3 mixing ratio between the surface and 12 km at three sites were between 20 and 40 ppbv and between 30 and 55 ppbv, respectively. An O_3-enhanced layer was defined by O_3 mixing ratios in excess of the lower 83.3% percentile range at each altitude. At the three sites, the occurrence of O_3-enhanced layers was about 50% on yearly average, indicating that O_3-enhanced layers occur frequently over the equatorial region. The occurrence shows a seasonal variation. At Watukosek, it was about 40% in the period from January to April and August to November, while it exceeded 70% in the other months. At

ACPD
7, 17179–17211, 2007

Samoa, it was less than 40% between February and April, while it was generally 50% or more from May to January except for in August. At San Cristobal, it was less than 30% in April, May and July, while it generally exceeded 50% in other months.

O_3 photochemical production following biomass burning is one of the processes by which O_3-enhanced layers are formed. Based on satellite hot-spot data, the OLR data and backward trajectory analyses, the contribution of biomass burning was estimated to be relatively high (about 30%) at San Cristobal during the periods from February to April and August to September, probably due to the influence of biomass burning in South America. In contrast, it was relatively low (about 10%) at Watukosek and Samoa. The latter result is at least partly because La Niña or La Niña-like conditions prevailed in the data period (between 1998 and 2002). During La Niña periods, biomass burning was inactive over the western Pacific region including Indonesia. Another significant process for the formation of O_3-enhanced layers is the transport of midlatitude UT/LS air. A major part of O_3-enhanced layers occurred with very low-RH, indicating downward displacement of the air masses and/or transport of dry air masses. Backward trajectory analyses showed that numerous dry, O_3-enhanced air masses were transported from latitudes higher than 25° around the subtropical jet stream region and from altitudes higher than the 300 hPa level. This process significantly contributed to the formation of O_3-enhanced layers in the equatorial Pacific region. The contribution of this process was relatively high, more than about 40% at Watukosek between May and December and about 60% or more at Samoa all year around, and about 40% or more between November and March and significant between August and September at San Cristobal. This process was important for the O_3 budget over the equatorial Pacific Ocean.

The transport process of the midlatitude UT/LS air toward the equatorial region has been revealed by meteorological analyses including PV and trajectories. Forward trajectories calculated from the region of |PV|=1 PVU show that the midlatitude UT/LS air masses were drawn out from relatively narrow region between high- and low-pressure systems in the upper troposphere near the subtropical jet stream and transported to the

ACPD
7, 17179–17211, 2007
Ozone-enhanced layers in the equatorial troposphere
H. Hayashi et al.

EGU

equatorial region. These meteorological characteristics and the transportation process were analogous to those of the intrusion of stratospheric air in the midlatitude (Palmen and Newman, 1969) in association with Rossby wave breaking. Previous studies showed that the midlatitude UT/LS air masses with high |PV| values are often transported to the subtropical and tropical latitudes around 20° (e.g., Baray et al., 1998), whereas they do not reach equatorial region directly. This study shows that the midlatitude UT/LS air is often transported to equatorial region to form dry, O_3-enhanced layers. The meteorological conditions causing the transport of midlatitude UT/LS air masses toward Watukosek and San Cristbal differed by season, and this difference was connected to the seasonal variation of the occurrence of O_3-enhanced layers.

To evaluate the contribution of the transport of midlaitude UT/LS air to the tropical tropospheric O_3 budget, additional analyses similar to this study using long-term observational data over other equatorial regions such as the tropical Indian Ocean and Atlantic Ocean are necessary. In addition, a comparison with results of chemical transport models would be significant to examine whether this process has been fully incorporated into the model calculations.

Acknowledgements. The trajectory calculation program used in this paper was developed by Y. Tomikawa and K. Sato at National Institute of Polar Research, Japan.

References

Baray, J.-L., Ancellet, G., Taupin, F. G., Bessafi, M., Baldy, S., and Keckhut, P.: Subtropical tropopause break as a possible stratospheric source of ozone in the tropical troposphere, J. Atmos. Sol. Terr. Phys., 60, 27–36, 1998.

Baray, J.-L., Daniel, V., Ancellet, G., and Legras, B.: Planetary-scale tropopause folds in the southern subtropics, Geophys. Res. Lett., 27, 353–356, 2000.

Chandra, S., Ziemke, J. R., Min, W., and Read, W. G.: Effects of 1997–1998 El Niño on tropospheric ozone and water vapor, Geophys. Res. Lett., 25, 3867–3870, 1998.

Fujiwara, M., Kita, K., and Ogawa, T.: Stratosphere-troposphere exchange of ozone associ-

ated with the equatorial Kelvin wave as observed with ozonesondes and rawinsondes, J. Geophys. Res., 103, 19 173–19 182, 1998.
Fujiwara, M., Kita, K., Kawakami, S., Ogawa, T., Komala, N., Saraspriya, S., and Suripto, A.: Tropospheric ozone enhancements during the Indonesian forest fire events in 1994 and in 1997 as revealed by ground-based observations, Geophys. Res. Lett., 26, 2417–2420, 1999.
Fujiwara, M., Kita, K., Ogawa, T., Kawakami, S., Sato, T., Komala, N., Saraspriya, S., and Suripto, A.: Seasonal variation of tropospheric ozone in Indonesia revealed by 5-year ground-based observations, J. Geophys. Res., 105, 1879–1888, 2000.
Fujiwara, M., Tomikawa, Y., Kita, K., Kondo, Y., Komala, N., Saraspriya, S., Manik, T., Suripto, A., Kawakami, S., Ogawa, T., Kelana, E., Suhardi, B., Harijono, S. W. B., Kudsy, M., Sribimawati, T., and Yamanaka, M. D.: Ozonesonde observations in the Indonesian maritime continent: a case study on ozone rich layer in the equatorial upper troposphere, Atmos. Environ., 37, 353–362, 2003.
Kita, K., Fujiwara, M., and Kawakami, S.: Total ozone increase associated with forest fires over the Indonesian region and its relation to the El Niño-southern oscillation, Atmos. Environ., 34, 2681–2690, 2000.
Kita, K., Kawakami, S., Miyazaki, Y., Higashi, Y., Kondo, Y., Nishi, N., Koike, M., Blake, D. R., Machida, T., Sato, T., Hu, W., Ko, M., and Ogawa, T.: Photochemical production of ozone in the upper troposphere in association with cumulus convection over Indonesia, J. Geophys. Res., 107, 8400, doi:10.1029/2001JD000844, 2002.
Kiladis, G. N.: Observations of Rossby waves linked to convection over the eastern tropical Pacific, J. Atmos. Sci., 55, 321–339, 1998.
Komala, N., Saraspriya, S., Kita, K., and Ogawa, T.: Tropospheric ozone behavior observed in Indonesia, Atmos. Environ., 30, 1851–1856, 1996.
Miloshevich, L. M., Vömel, H., Paukkunen, A., Heymsfield, A. J., and Oltmans, S. J.: Characterization and correction of relative humidity measurements from Vaisala RS80-A radiosondes at cold temperatures, J. Atmos. Ocean. Tech., 18, 135–156, 2001.
Newell, R. E., Wu, Z.-X., Zhu, Y., Hu, W., Browell, E. V., Gregory, G. L., Sachse, G. W., Collins, J. E. Jr., Kelly, K. K., and Liu, S. C.: Vertical fine-scale atmospheric structure measured from NASA DC-8 during PEM-West A, J. Geophys. Res., 101, 1943–1960, 1996.
Oltmans, S. J., Johnson, B. J., Harris, J. M., Vömel, H., Thompson, A. M., Koshy, K., Simon, P., Bendura, R. J., Logan, J. A., Hasebe, F., Shiotani, M., Kirchhoff, V. W. J. H., Maata, M.,

Sami, G., Samad, A., Tabuadravu, J., Enriquez, H., Agama, M., Cornejo, J., and Paredes, F.: Ozone in the Pacific tropical troposphere from ozonesonde observations, J. Geophys. Res., 106, 32 503–32 525, 2001.
Palmen, E. and Newton, C. W.: Atmospheric Circulation Systems, Academic Press, London, 603 pp., 1969.
Postel, G. A. and Hitchman, M. H.: A climatology of Rossby wave breaking along the subtropical tropopause, J. Atmos. Sci., 56, 359–373, 1999.
Scott, R. K., Cammas, J.-P., Mascart, P., and Stolle, C.: Stratospheric filamentation into the upper tropical troposphere, J. Geophys. Res., 106, 11 835–11 848, 2001.
Stoller, P., Cho, J. Y. N., Newell, R. E., Thouret, V., Zhu, Y., Carroll, M. A., Albercook, G. M., Anderson, B. E., Barrick, J. D. W., Browell, E. V., Gregory, G. L., Sachse, G. W., Vay, S., Bradshaw, J. D., and Sandholm, S.: Measurements of atmospheric layers from the NASA DC-8 and P-3B aircraft during PEM-Tropics A, J. Geophys. Res., 104, 5745–5764, 1999.
Thompson, A. M., Witte, J. C., McPeters, R. D., Oltmans, S. J., Schmidlin, F. J., Logan, J. A., Fujiwara, M., Kirchhoff, V. W. J. H., Posny, F., Coetzee, G. J. R., Hoegger, B., Kawakami, S., Ogawa, T., Johnson, B. J., Vömel, H., and Labow, G.: Southern Hemisphere Additional Ozonesondes (SHADOZ) 1998–2000 tropical ozone climatology 1. Comparison with Total Ozone Mapping Spectrometer (TOMS) and ground-based measurements, J. Geophys. Res., 108(D2), 8238, doi:10.1029/2001JD000967, 2003a.
Thompson, A. M., Witte, J. C., Oltmans, S. J., Schmidlin, F. J., Logan, J. A., Fujiwara, M., Kirchhoff, V. W. J. H., Posny, F., Coetzee, G. J. R., Hoegger, B., Kawakami, S., Ogawa, T., Fortuin, J. P. F., and Kelder, H. M.: Southern Hemisphere Additional Ozonesondes (SHADOZ) 1998–2000 tropical ozone climatology 2. Tropospheric variability and the zonal wave-one, J. Geophys. Res., 108(D2), 8241, doi:10.1029/2002JD002241, 2003b.
Thouret, V., Cho, J. Y. N., Evans, M. J., Newell, R. E., Avery, M. A., Barrick, J. D. W., Sachse, G. W., and Gregory, G. L.: Tropospheric ozone layers observed during PEM-Tropics B, J. Geophys. Res., 106, 32 527–32 538, 2001.
Tomikawa, Y. and Sato, K.: Design of the NIPR trajectory model, Polar Meteorol. Glaciol., 19, 120–137, 2005.
Waugh, D. W.: Impact of potential vorticity intrusions on subtropical upper tropospheric humidity, J. Geophys. Res., 110, D11305, doi:10.1029/2004JD005664, 2005.
Waugh, D. W. and Funatsu, B. M.: Intrusions into the tropical upper troposphere: Three-dimensional structure and accompanying ozone and OLR distributions, J. Atmos. Sci., 60,

637–653, 2003.
Waugh, D. W. and Polvani, L. M.: Climatology of intrusions into the tropical upper troposphere, Geophys. Res. Lett., 27, 3857–3860, 2000.
Yonemura, S., Tsuruta, H., Kawashima, S., Sudo, S., Peng, L. C., Fook, L. S., Johar, Z., and Hayashi, M.: Tropospheric ozone climatology over Peninsular Malaysia from 1992 to 1999, J. Geophys. Res., 107(D15), doi:10.1029/2001JD000993, 2002a.
Yonemura, S., Tsuruta, H., Maeda, T., Kawashimi, S., Sudo, S., and Hayashi, M.: Tropospheric ozone variability over Singapore from August 1996 to December 1999, Atmos. Environ., 36, 2061–2070, 2002b.
Yoneyama, K. and Parsons, D. B.: A proposed mechanism for the intrusion of dry air into the tropical western Pacific region, J. Atmos. Sci., 56, 1524–1546, 1999.
Zachariasse, M., Smit, H. G. J., van Velthoven, P. F. J., and Kelder, H.: Cross-tropopause and interhemispheric transports into the tropical free troposphere over the Indian Ocean, J. Geophys. Res., 106, 28 441–28 452, 2001.

ACPD
7, 17179–17211, 2007

Title Page
Abstract Introduction
Conclusions References
Tables Figures
◀ ▶
Back Close
Full Screen / Esc
Printer-friendly Version
Interactive Discussion

EGU

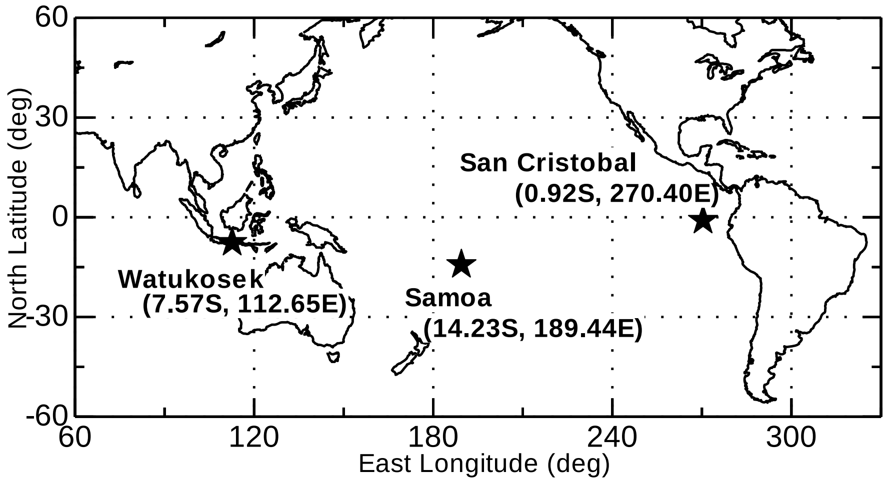

Fig. 1. The locations of the three ozonesonde stations, Watukosek, Samoa and San Cristobal, are indicated by stars.

ACPD
7, 17179–17211, 2007

Ozone-enhanced layers in the equatorial troposphere

H. Hayashi et al.

EGU

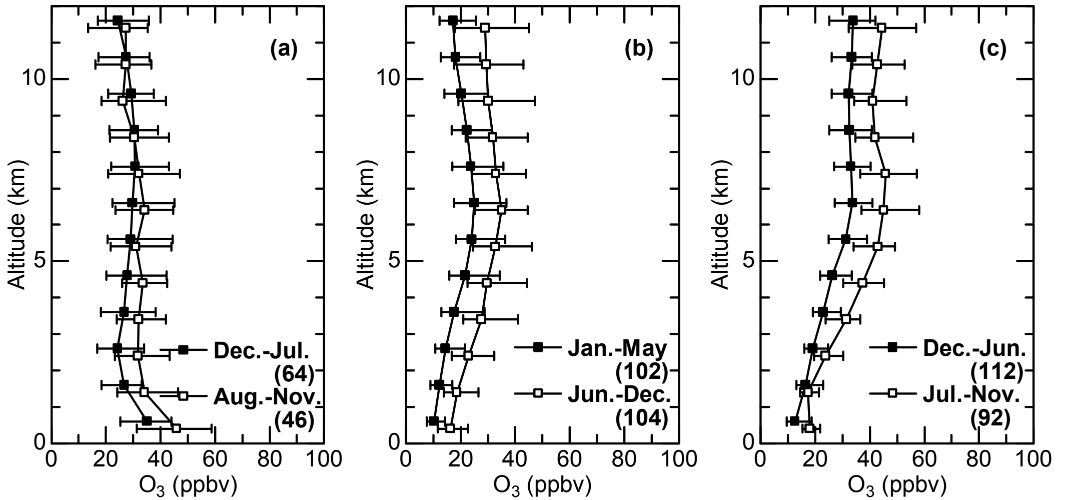

Fig. 2. Vertical profiles of median ozone mixing ratios at **(a)** Watukosek, **(b)** Samoa and **(c)** San Cristobal. Black and white squares indicate median values in two different periods of the year. The horizontal bars indicate the central 66.6% range for each 1-km altitude range. The numbers in parentheses are the numbers of observational data used for calculating median values in each period.

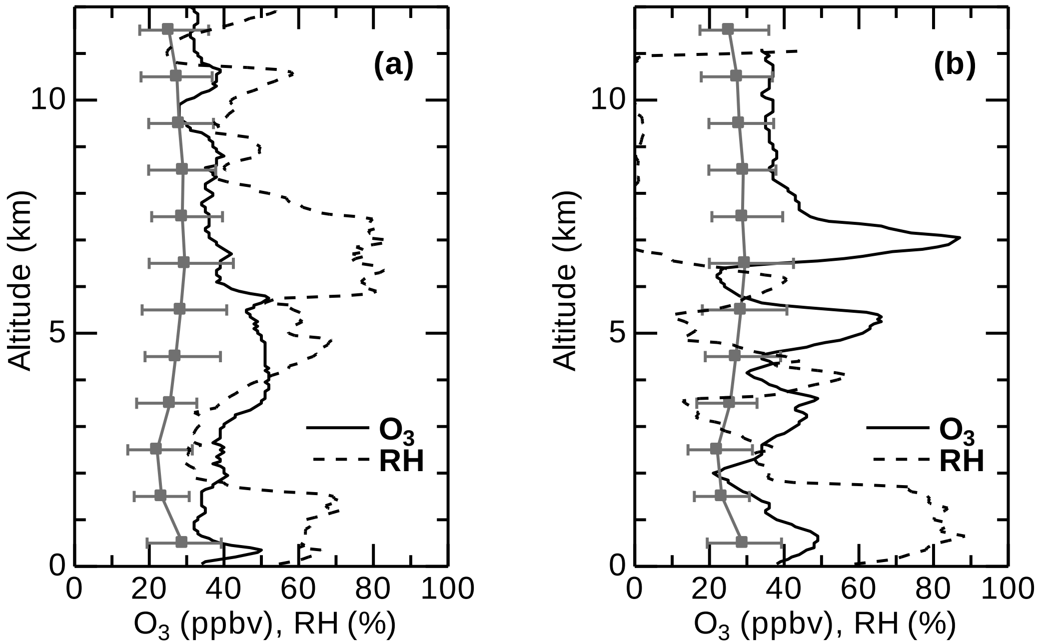

Fig. 3. Vertical profiles of O_3 mixing ratio (solid line) and relative humidity (dashed line) at Watukosek **(a)** on 3 December 2000, and **(b)** on 7 June 2000. The median values of the O_3 mixing ratios in the period from December to July are shown by gray squares, and their central 66.6% ranges are shown by horizontal bars.

ACPD
7, 17179–17211, 2007

Title Page
Abstract Introduction
Conclusions References
Tables Figures
◀◀ ▶▶
◀ ▶
Back Close
Full Screen / Esc
Printer-friendly Version
Interactive Discussion

EGU

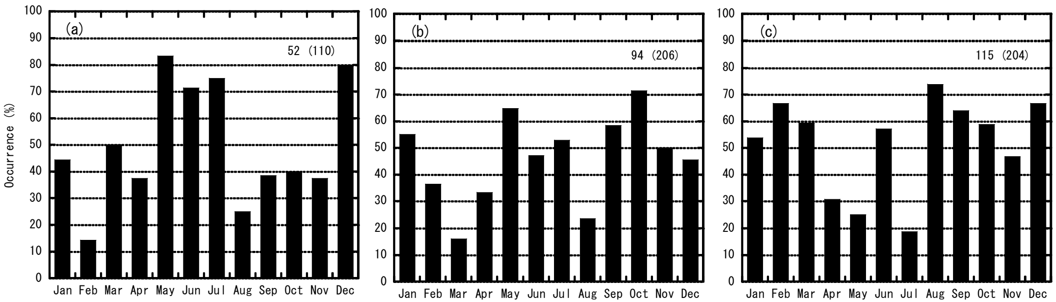

Fig. 4. Occurrence of tropospheric O_3-enhanced layers at **(a)** Watukosek, **(b)** Samoa and **(c)** San Cristobal by month. The number shown in the upper right of each panel is the number of O_3 profiles with O_3-enhanced layers in the whole data period, and the number in parenthesis is the total number of observed O_3 profiles.

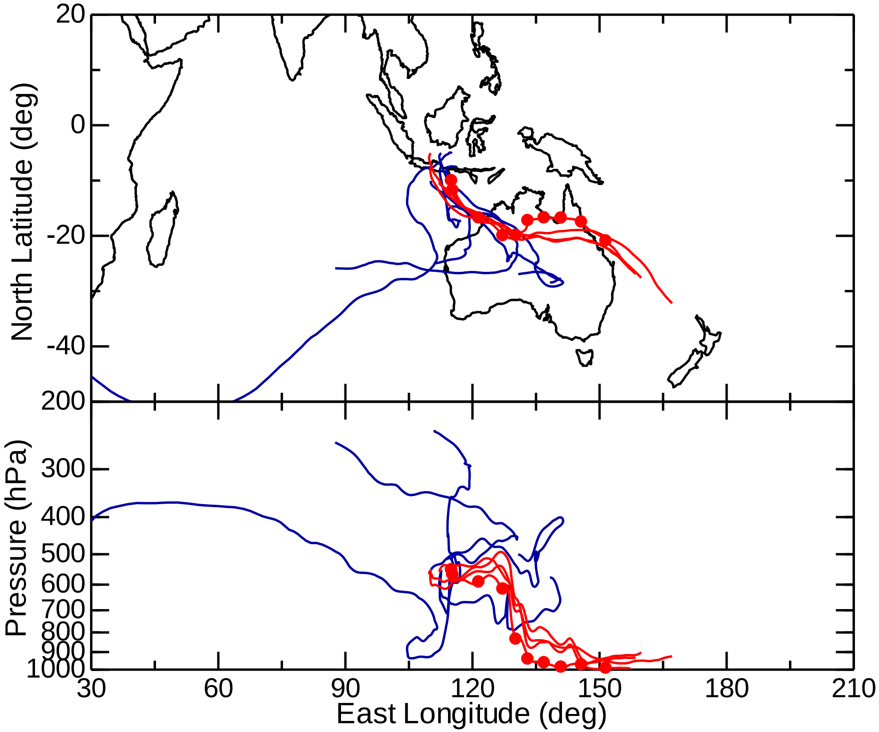

Fig. 5. Ten-day backward trajectories from Watukosek at 550 hPa on 3 December 2000. The trajectories were calculated from 9 grid points, and the center of the grid points was over Watukosek. The spatial interval of the grid points was 2.5° in latitude by 2.5° in longitude. Upper and lower panels show the horizontal and vertical motion of air masses, respectively. Dots show the air mass position on a representative trajectory in each 24-h interval.

ACPD
7, 17179–17211, 2007

EGU

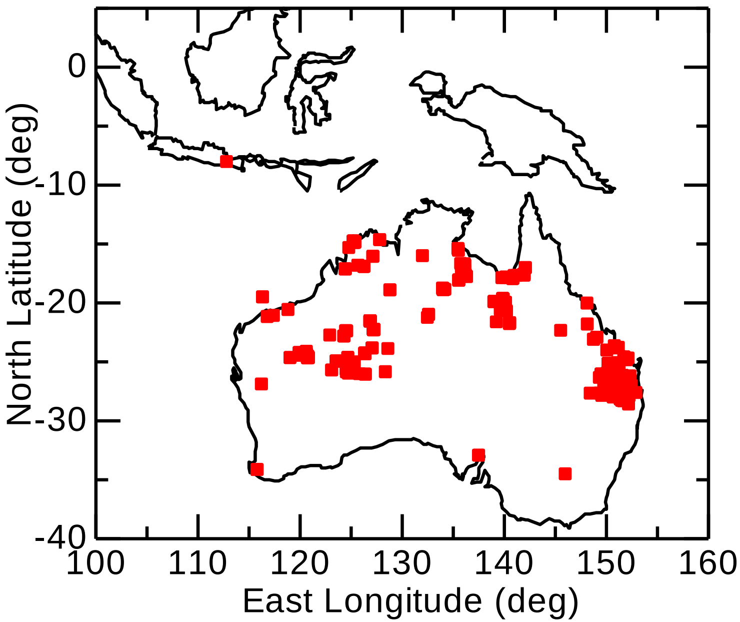

Fig. 6. The hot-spot distribution derived from the European Space Agency World Fire Atlas for the period from 24 November to 30 November 2000.

ACPD
7, 17179–17211, 2007

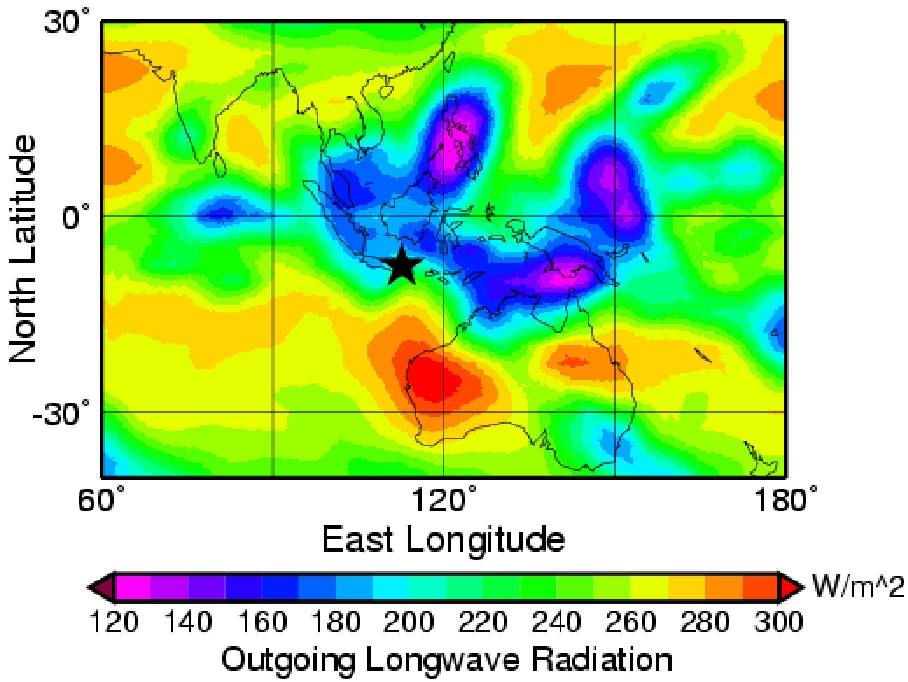

Fig. 7. A contour map of the daily average OLR value on 30 November 2000. The color bar refers to the OLR values in $W\,m^{-2}$.

ACPD
7, 17179–17211, 2007

Ozone-enhanced layers in the equatorial troposphere

H. Hayashi et al.

EGU

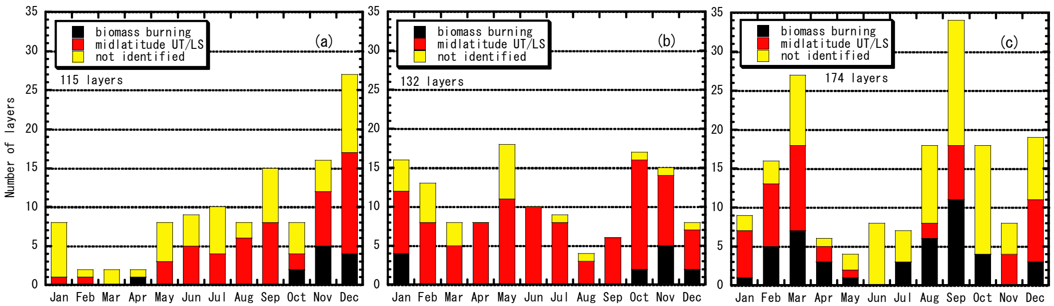

Fig. 8. Number of O_3-enhanced layers by month at **(a)** Watukosek, **(b)** Samoa and **(c)** San Cristobal. Black bars and red bars indicate the number of layers resulting from biomass burning and the transport of midlatitude UT/LS air, respectively. Yellow bars show the number of layers whose formation process was not identified. The number shown in each panel is the total number of O_3-enhanced layers.

ACPD

7, 17179–17211, 2007

Title Page

Abstract | Introduction

Conclusions | References

Tables | Figures

◀◀ | ▶▶

◀ | ▶

Back | Close

Full Screen / Esc

Printer-friendly Version

Interactive Discussion

EGU

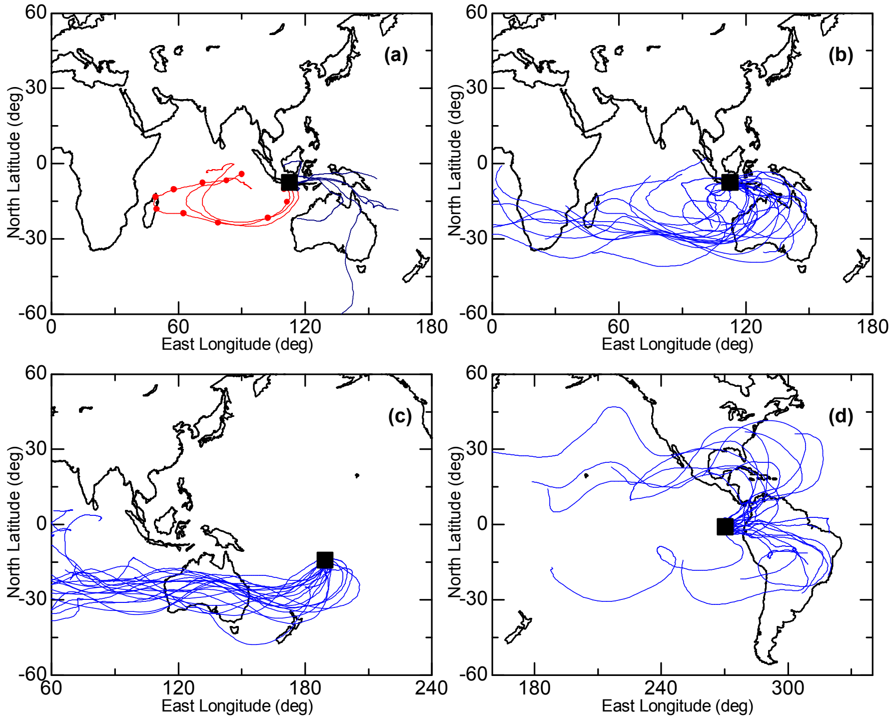

Fig. 9. Ten-day backward trajectories from the altitude of O_3-enhanced layers with low relative humidity. **(a)** Trajectory from Watukosek on 7 June. Dots show the air mass position on a representative trajectory in each 24-h interval. **(b)**, **(c)** and **(d)** Twenty representative trajectories tracing back to the subtropical jet stream region from Watukosek, Samoa, and San Cristobal, respectively.

ACPD
7, 17179–17211, 2007

H. Hayashi et al.

Title Page
Abstract | Introduction
Conclusions | References
Tables | Figures
◀| |▶
◀ ▶
Back | Close
Full Screen / Esc
Printer-friendly Version
Interactive Discussion

EGU

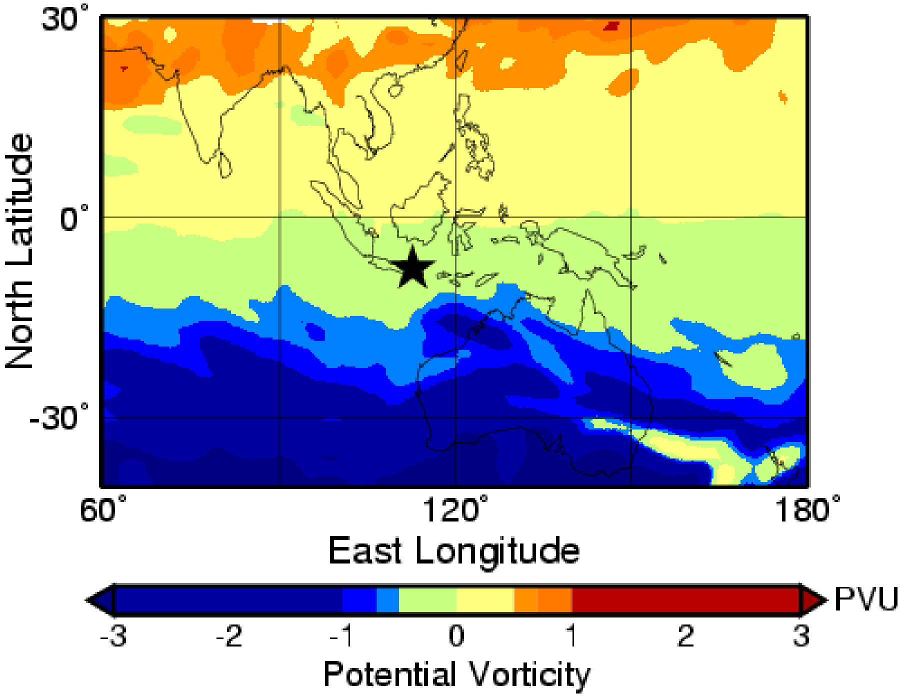

Fig. 10. A contour map of PV on the 327 K isentropic surface on 5 June 2000. Location of Watukosek is indicated by a star. The color bar indicates the PV values in PVU.

ACPD
7, 17179–17211, 2007

EGU

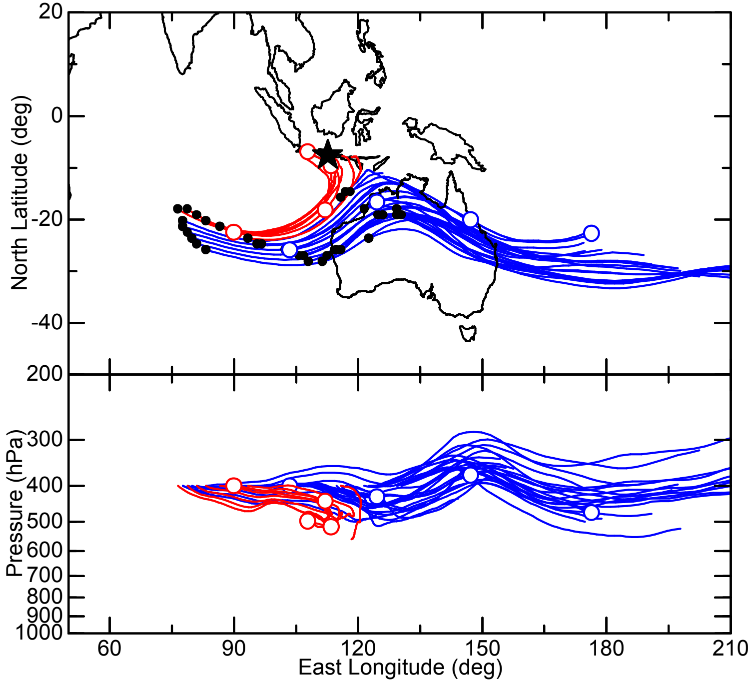

Fig. 11. Three-day forward trajectories calculated from the region of PV=−1 PVU shown in Fig. 10 on the 327 K isentropic surface on 5 June 2000. White dots indicate the air mass position on representative trajectories in each 24-h interval.

ACPD
7, 17179–17211, 2007

Title Page
Abstract | Introduction
Conclusions | References
Tables | Figures
Back | Close
Full Screen / Esc
Printer-friendly Version
Interactive Discussion

EGU

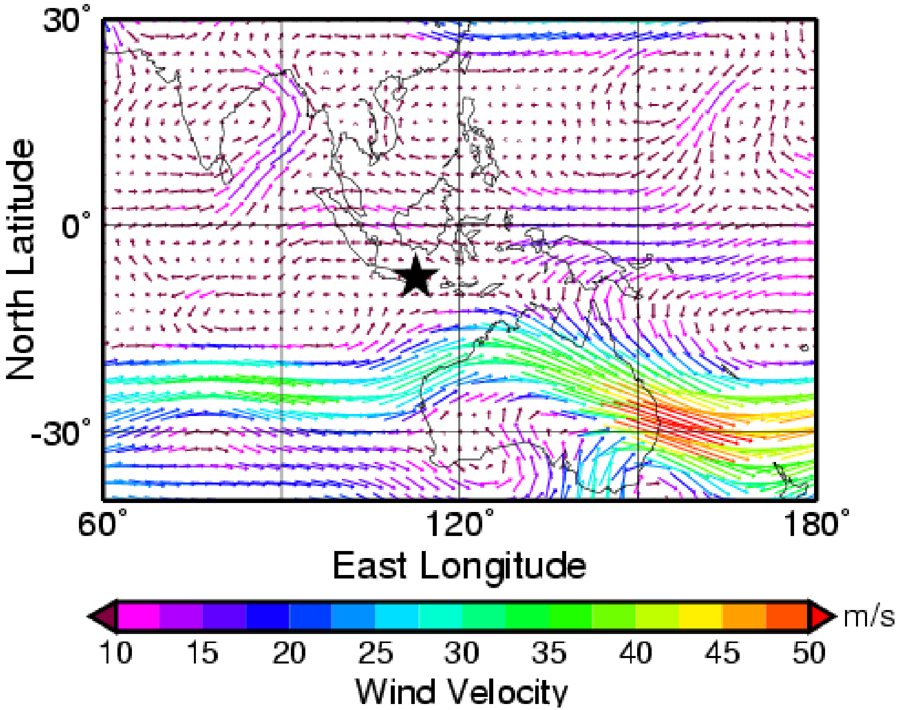

Fig. 12. A map indicating the daily average values of horizontal wind vectors at 400 hPa on 5 June 2000. The wind data were obtained from the NOAA-CIRES Climate Diagnostics Center (http://www.cdc.noaa.gov/Composites/Day/). The color bar indicates the horizontal wind velocity in m s^{-1}.

ACPD
7, 17179–17211, 2007

Ozone-enhanced layers in the equatorial troposphere

H. Hayashi et al.

EGU

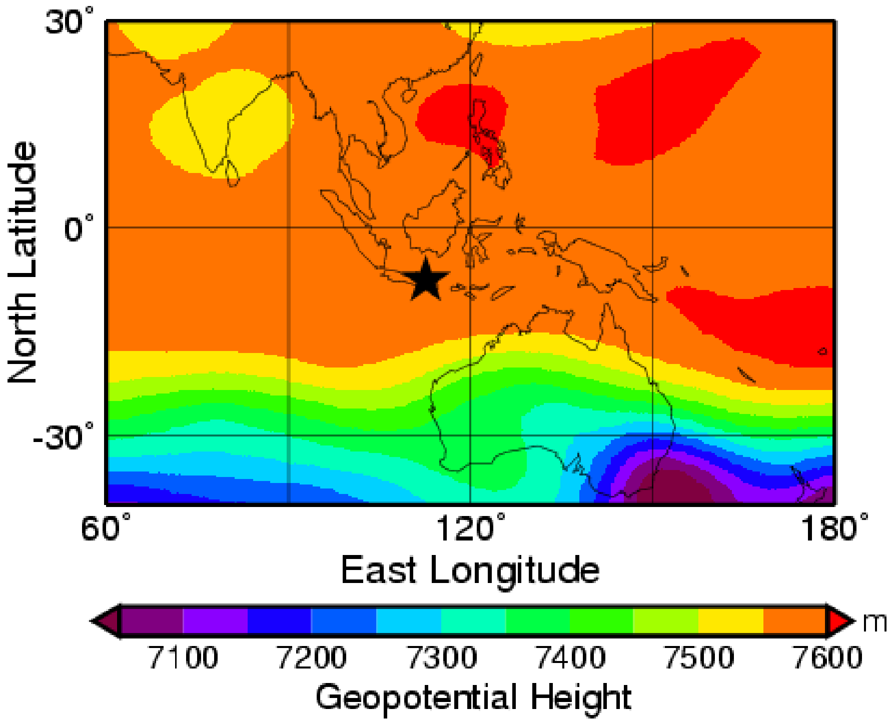

Fig. 13. A contour map indicating the daily average value of the geopotential height at 400 hPa on 5 June 2000. The data were obtained from the NOAA-CIRES Climate Diagnostics Center (http://www.cdc.noaa.gov/Composites/Day/). The color bar indicates the geopotential height value in m.

ACPD
7, 17179–17211, 2007

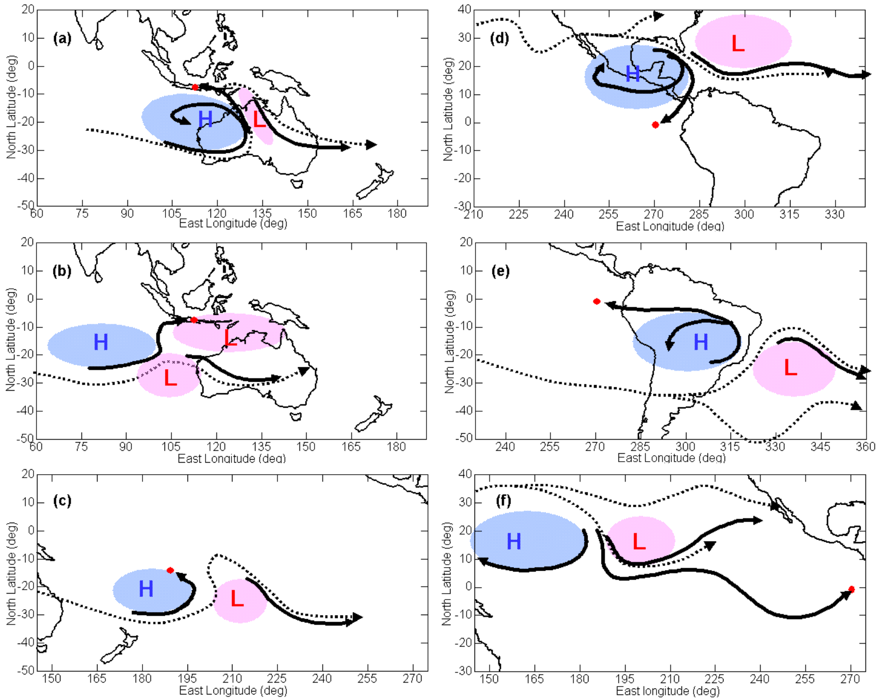

Fig. 14. Schematic illustrations of the transport processes of midlatitude UT/LS air masses to the equatorial Pacific region: **(a)** for Watukosek in the dry season, between May and October; **(b)** for Watukosek in the wet season, between November and December; **(c)** for Samoa all year around; **(d)** for San Cristobal in the period from August to September; **(e)** for San Cristobal in the period from February to March; and **(f)** for San Cristobal in the period from November to January. Solid curves with arrows are representative examples of the forward trajectories indicating motions of |PV|=1 PVU air masses. Red dots and dotted curves with arrows indicate the position of observational sites and the schematic path of the jet stream, respectively. The signs "H" and "L" indicate the rough positions of the high- and low-pressure systems affected the transport of midlatitude UT/LS air masses to the observational sites.

ACPD

7, 17179–17211, 2007

Ozone-enhanced layers in the equatorial troposphere

H. Hayashi et al.

EGU